




# Hydrothermal carbonization of *Spirogyra* sp. algae for adsorption and regeneration of malachite green dye

Muhammad Badaruddin <sup>a</sup>, Laila Hanum <sup>c</sup>, Elda Melwita <sup>b</sup> ,  
Sahrul Wibiyana <sup>bd</sup> , Aldes Lesbani <sup>bd \*</sup> 

- a:** Doctoral Program of Environmental Science, Postgraduate Program, Universitas Sriwijaya, Palembang 30139, South Sumatera, Indonesia  
**b:** Master Program of Materials Science, Graduate School, Universitas Sriwijaya, Palembang 30139, South Sumatera, Indonesia  
**c:** Biology Department, Faculty of Mathematics and Natural Sciences, Universitas Sriwijaya, Indralaya 30662, Indonesia  
**d:** Research Center of Inorganic Materials and Coordination Complexes, Universitas Sriwijaya, Palembang 30139, Indonesia  
\* Corresponding author: [aldeslesbani@pps.unsri.ac.id](mailto:aldeslesbani@pps.unsri.ac.id)



## Abstract

In this study, we prepared hydrochar (HCSP) from *Spirogyra* sp. algae (SP) as adsorbent to eliminate malachite green (MG) dye and conducted the adsorbent regeneration study. SP and HCSP were characterized using FTIR, XRD, SEM, and BET. The adsorption performance was evaluated under various conditions of pH, contact time, concentration, and temperature. SP and HCSP were optimum at pH 8 for MG adsorption. The suitable adsorption kinetics model was PSO, and the adsorption isotherm model tended to be the Freundlich model. The maximum adsorption capacity ( $Q_{max}$ ) obtained from Langmuir calculation at 30 °C, SP and HCSP were 34.96 mg/g and 99.01 mg/g, respectively. The thermodynamic parameters indicated endothermic and spontaneous processes, with HCSP exhibiting greater adsorption capacity and spontaneity than SP. Regeneration studies demonstrated that HCSP and SP materials could be reused up to the 4<sup>th</sup> cycle with the remaining efficiency of 69.37% and 49.30%, respectively. Compared to SP, HCSP has better adsorption capacity.

## Key findings

- Hydrothermal carbonization produced porous *Spirogyra* sp. hydrochar, ideal for adsorption applications.
- The adsorbent showed excellent regeneration, enabling effective reuse with maintained adsorption performance.
- The adsorption involves electrostatic interaction, hydrogen bonding, and  $\pi$ - $\pi$  interactions at the functional groups.

© 2024, the Authors. This article is published in open access under the terms and conditions of the Creative Commons Attribution (CC BY) license (<http://creativecommons.org/licenses/by/4.0/>).

## 1. Introduction

Synthetic dyes are often used in various industrial fields, including the textile industry, paints, and paper mills, but their effluents pose significant environmental and health risks [1]. These effluents contain toxic and carcinogenic contaminants that can be released into waterways in soluble or insoluble forms. When these dyes interact with metal ions, they produce substances that are highly toxic to aquatic flora and fauna, leading to various diseases [2, 3].

One of such toxic dyes is malachite green. The complex structure of malachite green makes it resistant to

decomposition by chemicals, enzymes, oxidizing agents and heat, leading to ecosystem damage. In wastewater treatment, malachite green is difficult to remove due to its chemical stability. Human health is also threatened as these dyes can enter the food chain, causing mutagenesis, allergic reactions, and carcinogenic effects. Hence, the extensive use of synthetic dyes in industry has a negative impact on the environment and human health, necessitating better waste management practices [4, 5].

Methods for treating dye effluents include physical, chemical, biological, and hybrid methods. Physical methods commonly used to remove pollutants are adsorption,

## Accompanying information

### Article history

Received: 07.11.24

Revised: 20.12.24

Accepted: 21.12.24

Available online: 26.12.24

### Keywords

algae, *spirogyra* sp., hydrochar, hydrothermal carbonization, regeneration

### Funding

None.

### Supplementary information

Transparent peer review: 

### Sustainable Development Goals



membrane filtration, coagulation, and ion exchange. Chemical methods commonly used to remove pollutants include ozonation, Fenton reagent, electro-chemical deconstruction, and photocatalysis processes. Biological processes use microorganisms or enzymes. Adsorption is considered the most superior method due to its productivity in removing contaminants through surface-based phenomena that attract atoms, molecules, or ions on the surface of solids. Adsorption is used for textile effluent treatment because the adsorption mechanism can be utilised for the degradation of dissolved organic impurities, such as dyes and colourants [6]. Methods for textile dye wastewater purification include adsorption, biodegradation, and advanced oxidation processes [7].

Hydrochar, also known as charcoal synthesized by hydrothermal carbonization (HTC), both natural and modified, is effective in removing colorants through mechanisms such as precipitation, surface complexation, and electrostatic attraction [8, 9]. Agricultural waste (orange peels, coconut shells, pine sawdust, as well as sewage sludge) is one of the many biomass sources from which hydrochar can be made. Hydrochar derived from agricultural waste such as persimmon peel [10] and pomegranate peel waste [11] showed high adsorption capacity for synthetic cationic dyes. Various other materials that can be used to remove dye pollutants from wastewater include clays/zeolites and their composites, biosorbents, chitosan, *Spirulina platensis*, and kaolin [12].

Hydrochar is a versatile material offering sustainable solutions to various environmental challenges. It is produced from biomass waste, such as cellulosic biopolymer waste, and exhibits excellent adsorption properties to remove dye contaminants from water [13, 14]. Hydrochar has several advantages compared to char produced by pyrolysis. First, the yield of hydrochar from HTC is higher due to the less complete decomposition of biomass during the process. In addition, the hydrochar from the leached biomass shows higher thermal stability compared to the hydrochar from the original biomass, which is due to the efficiency of HTC in dissolving minerals containing calcium and potassium. These minerals usually catalyze the char formation reaction under pyrolysis conditions, so their absence in the hydrochar improves the thermal stability of the final product. Hydrochar also has a larger surface area after the leaching process due to lower mineral content, which contributes to the improvement of product quality. Hydrochar from HTC has advantages in terms of yield, thermal stability, and surface area compared to char from pyrolysis [15].

The hydrochar preparation process generally involves hydrothermal carbonization (HTC), where biomass is heated in water at high temperature and high pressure, producing carbonaceous material. This process does not require additional activation to produce the base hydrochar, which already has better stability and characteristics compared to the initial feedstock [16]. *Spirogyra sp.* algae are used to make hydrochar because these two algae contain

high carbon sources so they have the potential to be made into hydrochar and used as adsorbents.

*Spirogyra sp.* is a type of algae that has been studied extensively for its diverse capabilities. Studies have shown that *Spirogyra sp.* algae can serve as bioindicators for heavy metal pollution in aquatic environments, accumulating metals such as manganese, copper, chromium, lead, and zinc [17]. The content of *Spirogyra sp.* is total protein  $16.7 \pm 1.5\%$  (range 12.0–24.4%), total carbohydrate  $55.7 \pm 2.4\%$  (range 42.8–62.0%), and total lipid  $18.1 \pm 0.7\%$  (range 14.8–21.0%) [18, 19]. The cell wall of *Spirogyra sp.* consists of several constituent compounds. *Spirogyra sp.* contains cellulose in its cell wall. The cell wall of *Spirogyra zygospores* has a helicoidal pattern of multilayered cellulose, algaenan, pectin, and other polysaccharides. Algaenan is a component resistant to acids and bases, often found in tri-laminar cell wall structures in freshwater microalgae. Pectin, particularly homogalacturonan with a low degree of methyl esterification, was also found in *Spirogyra sp.* samples. In addition, protein arabinogalactans and xyloglucans are also part of the outer cell wall of *Spirogyra sp.* The cell wall characteristics of *Spirogyra sp.* can be considered resilient for several reasons supported by its various constituent components. The *Spirogyra sp.* cell wall consists of several layers containing various polysaccharides including cellulose and pectin, which give the cell wall structure strength and flexibility. In addition, the presence of algaenan, which is a heteropolymer polyester that is highly resistant to acids and bases, also contributes to the resilience and ductility of the cell wall [20, 21].

We conducted research on *Spirogyra sp.* as a basic material for making hydrochar as a dye adsorbent because this algae is rich in compounds that have the potential to support the adsorption process. *Spirogyra sp.* contains high levels of polysaccharides, proteins, lipids, and cellulose fibres, which serve as active groups in the binding of pollutant molecules. The content and characteristics of *Spirogyra sp.* algae is the reason for researchers to make it into hydrochar with the assumption that it can produce hydrochar which has good adsorption and regeneration capacity.

## 2. Experimental Section

### 2.1. Chemicals and Instrumentation

The chemicals used in this study include sodium hydroxide (NaOH), hydrochloric acid (HCl), distilled water (H<sub>2</sub>O) and cationic dye malachite green. The sample of *Spirogyra sp.* algae obtained from Lebung Jangkar Village, Pemulutan District, Ogan Ilir Regency, South Sumatra Province ( $-3.113052^\circ, 104.786218^\circ$ ).

The tools used in this research are standard laboratory glassware and instrumentation equipment consisting of Hydrothermal Stainless-steel Autoclave, microscope, Rigaku MiniFlex600 X-ray Diffraction (XRD), Shimadzu Prestige-21 Fourier Transform Infra-Red Spectroscopy (FTIR), Hitachi SU-3500 and Jeol JSM-IT200 No BMN

Scanning Electron Microscopy (SEM), Quantachrome type NovaWin Brunauer-Emmett-Teller (BET) Surface Area Analyzer, and EMC-18PC-UV Ultraviolet (UV)-Visible Spectrophotometer.

## 2.2. Algae *Spirogyra sp.* preparation

*Spirogyra sp.* algae sample were washed thoroughly using distilled water and identified using a microscope, then cut into small pieces and dried in an oven at 100 °C until dry, after which they were crushed and sieved using a 100 mesh sieve. The prepared materials were characterized using XRD, FT-IR, SEM and BET analysis.

## 2.3. Algae *Spirogyra sp.* hydrothermal carbonization

A total of 2.5 g of *Spirogyra sp.* algae preparation was added to 50 mL of distilled water, then put into a 100 mL Hydrothermal Stainless-steel Autoclave. The autoclave was put into the oven at 250 °C and then in the oven for 12 h, then cooled at room temperature and washed with distilled water, after which it was dried in the oven at 105 °C for 24 h. The hydrochar material obtained was pulverized using a mortar and sieved using a 100 mesh sieve, then characterized by XRD, FT-IR, SEM and BET.

## 2.4. Algae *Spirogyra sp.* hydrothermal carbonization

Determination of pH<sub>pzc</sub> was carried out by adding 0.02 g of each adsorbent into 20 mL of NaCl solution with a concentration of 0.1 M which has been adjusted to pH with variations of pH 2, 3, 4, 5, 6, 7, 8, 9, 10, and 11. The NaCl solution was pH-adjusted by adding NaOH and HCl solutions with a concentration of 0.1 M. The mixture was stirred for 24 h, then filtered and the filtrate was measured for final pH using a pH meter, and then a plot was made of the relationship between the initial pH and final pH.

## 2.5. Adsorption Procedure

The adsorption procedure was carried out with parameters such as pH of adsorps, time, and the effect of concentration and temperature to determine the best adsorption conditions of malachite green dye. The pH variation was carried out to determine the optimum adsorption in an acidic pH to alkaline pH environment from pH 2 to pH 11 using NaOH and HCl. The pH variation procedure uses 20 mL of malachite green dye with a concentration of 50 mg/L. The initial absorbance was measured using a UV-Vis spectrophotometer. Next, 0.02 g of adsorbent was added and stirred for 2 h, and the final absorbance was measured again. The time variation procedure to see the optimum time conditions for adsorption of malachite green dye with adsorption was carried out from 5 to 210 min where each time the absorbance was measured. The effect of concentration was analyzed by adding 0.02 g of adsorbent to 20 mL of malachite green dye

solution with concentrations of 20, 50, 100, and 200 mg/L and also varying the temperature at 30 °C, 40 °C, 50 °C, and 60 °C. The solution was stirred for the optimum time, then separated and measured the final absorbance.

## 2.6. Reuse of regeneration adsorbent

25 ml of malachite green dye with a concentration of 100 mg/L was put into a beaker, and the pH of the solution was adjusted to the optimal pH. Then 0.025 g adsorbent was added. The mixture was stirred with a magnetic stirrer during the optimal adsorption time. Then the separation process between adsorbent and adsorbate was carried out. The filtrate in the form of adsorbate was measured for absorbance with a UV-Vis spectrophotometer. The adsorbent obtained was then washed with distilled water and desorbed with the ultrasonic device. After drying, the resulting adsorbent was ready to be reused.

# 3. Result and Discussion

## 3.1. Characterization

### 3.1.1. Fourier transform infrared spectrophotometer

FTIR analysis of SP and HCSP materials can be seen in Figure 1 (a). The peak at 3412 cm<sup>-1</sup> is identified as O-H stretching and N-H groups which can be found in the materials. The materials have carboxyl and phenolic groups identified at the peak wave number of 2933 cm<sup>-1</sup>. The identification of C=O and O-H groups in the carboxyl and phenolic component is seen at 1645 cm<sup>-1</sup> and 1531 cm<sup>-1</sup>. The N-H group was identified as the peak at 1375 cm<sup>-1</sup>. The C-OH band vibration was identified at 1027 cm<sup>-1</sup>. The C-N-S shear in the material was identified at 528 cm<sup>-1</sup> derived from the polypeptide structure [22]. Some peaks in the HCSP material decreased which can be seen in Figure 1 (a). Examples of peaks that decreased are seen at 3412 cm<sup>-1</sup>, 2933cm<sup>-1</sup>, 1645 cm<sup>-1</sup>, 1027 cm<sup>-1</sup> and 528 cm<sup>-1</sup> indicating the reduction of hydroxyl functional groups derived from water content or N-H phenolic groups, so it is assumed that hydrochar was successfully synthesized [23].

### 3.1.2. X-Ray diffraction

The main peaks describing SP and HCSP materials can be seen in Figure 1(b) are 2θ around 23.28°, 26.64°, 29.45°, 36.17°, 43.81, 47.98°, 57.83°, 61.75° and 65.66°. These peaks match the JCPDS data (01-086-2334) which shows that the material is confirmed to have a phase similar to calcium carbonate or CaCO<sub>3</sub> [24]. In the HCSP material, there is a slight shift in the 2θ value and a new peak 2θ around 16.94° is assumed to be the increased ratio and formation of a more regular carbon structure, indicating the successful manufacture of hydrochar.

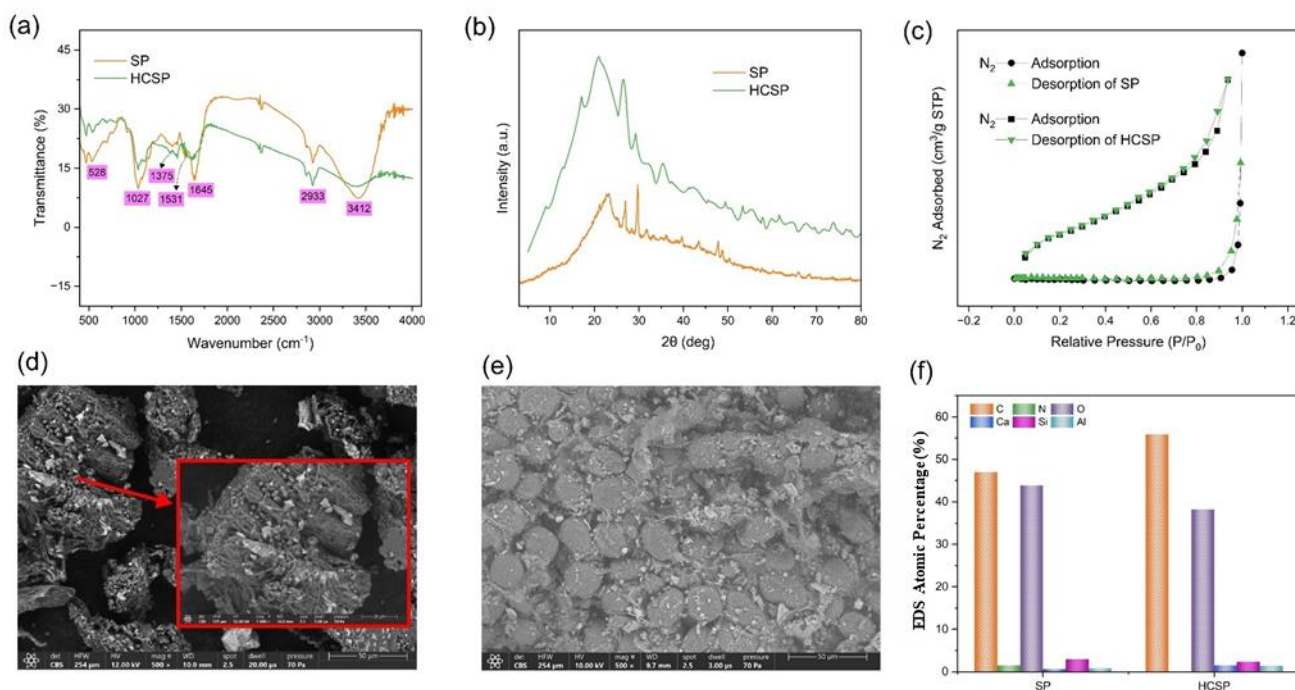


**Figure 1** The FTIR spectra (a), XRD pattern (b), BET N<sub>2</sub> adsorption-desorption (c) of SP and HCSP. SEM image of SP (d), HCSP (e) and EDS atomic fractions for SP and HCSP (f).

### 3.1.3. Scanning electron microscopy

Figure 1(d) shows the SEM image of SP. It is clearly seen at 1000x magnification that SP has a morphology in the form of filamentous fibers that are spiral-shaped from the chloroplast arrangement of *Spirogyra sp* [25]. After SP is made into hydrochar, namely HCSP in Figure 1(e), the surface morphology changes to the shape of granules forming porous materials which is characteristic of the hydrochar material [26, 27]. Figure 1(f) shows the atomic percentage of SP and HCSP materials. HCSP material has increased percentage of C to 55.9% as compared with 47% in the SP material. In addition, N disappeared in HCSP material, and there is Ca content in SP and HCSP material. This data supports the results of the previous FTIR and XRD analysis that the HCSP material has experienced water reduction and was converted into carbon material with the CaCO<sub>3</sub> phase with a more regular arrangement and a larger ratio. Si and Al contained in the materials were identified as coming from sedimentation in the *Spirogyra sp.* algae growing environment.

### 3.1.4. BET surface area analysis

The hysteresis curves of SP and HCSP materials show type IV(a) isotherm curves. The hysteresis curves of SP and HCSP materials can be seen in Figure 1(c). The materials that have type IV (a) isotherm curves have pore sizes of  $2 \text{ nm} \leq d \leq 50 \text{ nm}$  in the mesoporous range, which affects the way gas is adsorbed and desorbed by the material [28, 29]. Table 1 explains that HCSP has increased its surface area to  $5.50 \text{ m}^2/\text{g}$  from the initial SP material surface area of

$0.20 \text{ m}^2/\text{g}$ . This increase in surface area shows that adsorption can also be more effective.

### 3.2. pH<sub>pzc</sub> materials and effect of pH on adsorption

pH<sub>pzc</sub> (zero point charge) which can be seen in Figure 2(a) is the characteristic of the material at a certain pH when the material is uncharged, for example, an adsorbent that has a characteristic charge on its surface. pH<sub>pzc</sub> in adsorption is related to the adsorbate used. In the material below the optimum pH of adsorption the surface is positively charged; if the material is above the optimum pH of adsorption, the surface is negatively charged [30]. SP and HCSP materials have pH<sub>pzc</sub> at pH 6.65 and 6.72, while the optimum adsorption conditions for malachite green for SP and HCSP materials which can be seen in Figure 2(b) are above pH<sub>pzc</sub> with an optimum pH of 8, with adsorbed concentrations of  $42.83 \text{ mg/g}$  and  $46.18 \text{ mg/g}$ , indicating that SP and HCSP materials have a negative charge on their surface.

### 3.3. Effect of contact time on adsorption

The optimal time conditions (adsorption and kinetic parameters PFO and PSO) of SP and HCSP can be seen in Figure 2(c).

**Table 1** Surface area BET, pore size and pore volume of SP and HCSP.

Material	SBET (m <sup>2</sup> /g)	Average pore size (nm)	Average pore volume (cm <sup>3</sup> /g)
SP	0.20	87.63	2.69
HCSP	5.50	4.43	0.01



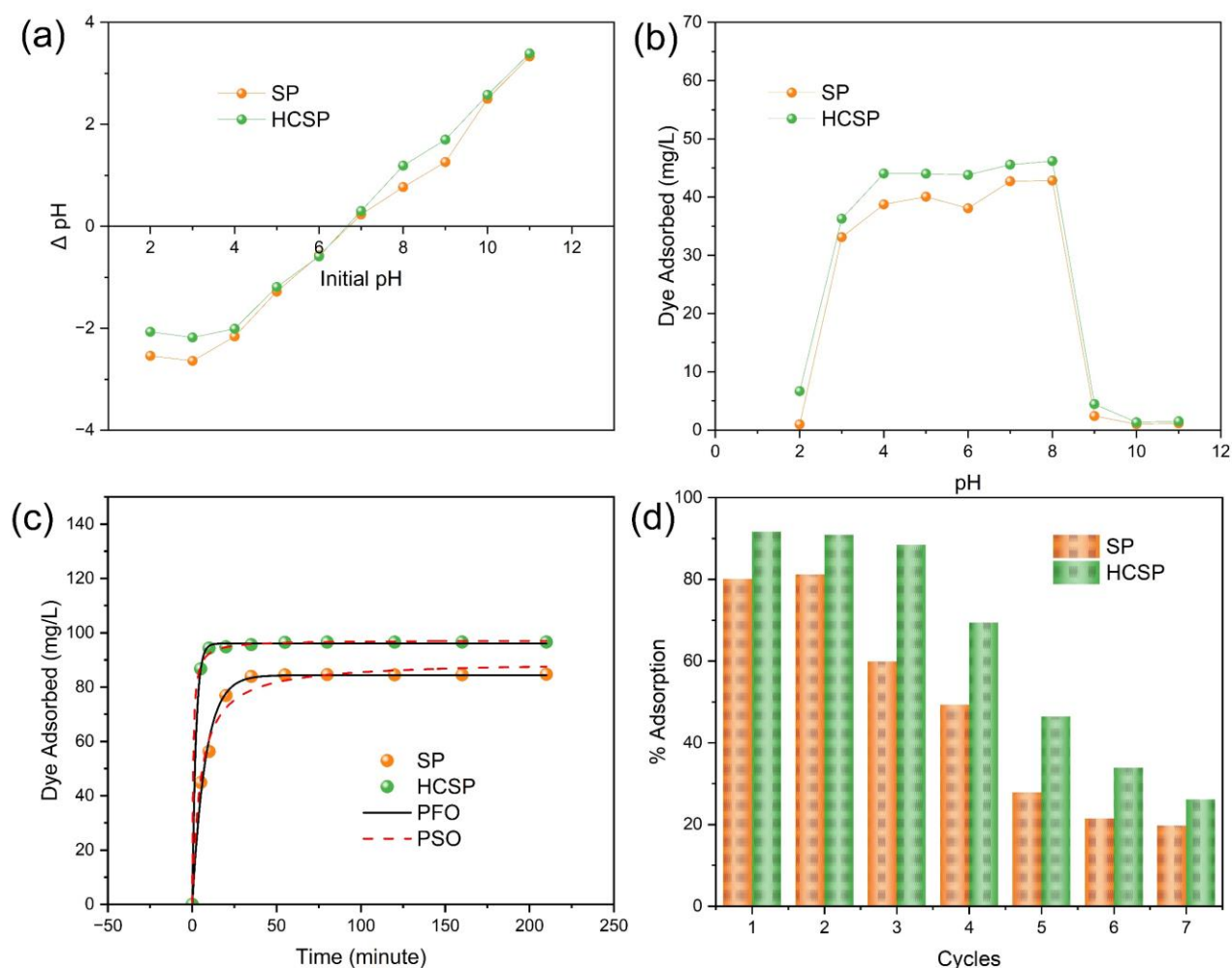


**Figure 2** The pH point zero charge (PZC) (a), effect of pH adsorption (b), effect of time adsorption and kinetic parameter (c) and regeneration cycles (d) of SP and HCSP.

**Table 2** The kinetic parameters PFO and PSO models of SP and HCSP.

Adsorbent	$Q_{e \text{ exp}}$ (mg/g)	Pseudo first order			Pseudo second order		
		$Q_{e \text{ calc}}$ (mg/g)	$k_1$ ( $\text{min}^{-1}$ )	$R^2$	$Q_{e \text{ calc}}$ (mg/g)	$k_2$ (g/mg)/min	$R^2$
SP	84.50	94.17	0.140	0.988	86.20	0.005	0.999
HCSP	96.44	84.99	0.383	0.987	97.09	0.035	1.000

HCSP material at the 5<sup>th</sup> minute successfully adsorbed malachite green dye of 86.70 mg/L, indicating that adsorption occurred quickly. At the 55<sup>th</sup> min the amount adsorbed reached 96.44 mg/L. SP material showed an optimum time of 55 min with adsorption of 84.50 mg/L. HCSP material has greater adsorption than SP, indicating hydrochar successfully increased the adsorption capability.

The analysis of Pseudo First Order (PFO) and Pseudo Second Order (PSO) adsorption kinetics models can be seen in Table 2. SP and HCSP materials tend to be more suitable for the PSO kinetics model as seen from the  $R^2$  value closer to 1. The experimental adsorption capacity ( $Q_{e \text{ exp}}$ ) in the PFO model shows SP and HCSP materials of 84.50 mg/g and 96.44 mg/g, not much different from the calculated adsorption capacity ( $Q_{e \text{ calc}}$ ) of PFO of 94.17 mg/g and 84.99 mg/g. In the PSO model, SP and HCSP materials have  $Q_{e \text{ calc}}$  of 86.20 mg/g and 97.09 mg/g.

### 3.4. Impact of concentration and temperature on adsorption

The model and graphic of isotherm Langmuir and Freundlich of the materials SP and HCSP can be seen in Figure 3 and Table 3. SP material showed  $R^2$  values in Langmuir and Freundlich isotherm models that did not differ much in value. HCSP material  $R^2$  value shows the adsorption isotherm model tends to the Freundlich model. This shows that adsorption that occurs on HCSP material tends to be multilayer. The maximum adsorption capacity of the Langmuir isotherm model at 30 °C of SP and HCSP materials of 34.96 mg/g and 99.01 mg/g proves that the manufacture of hydrochar is successfully carried out and increases the adsorption ability towards the malachite green dye.

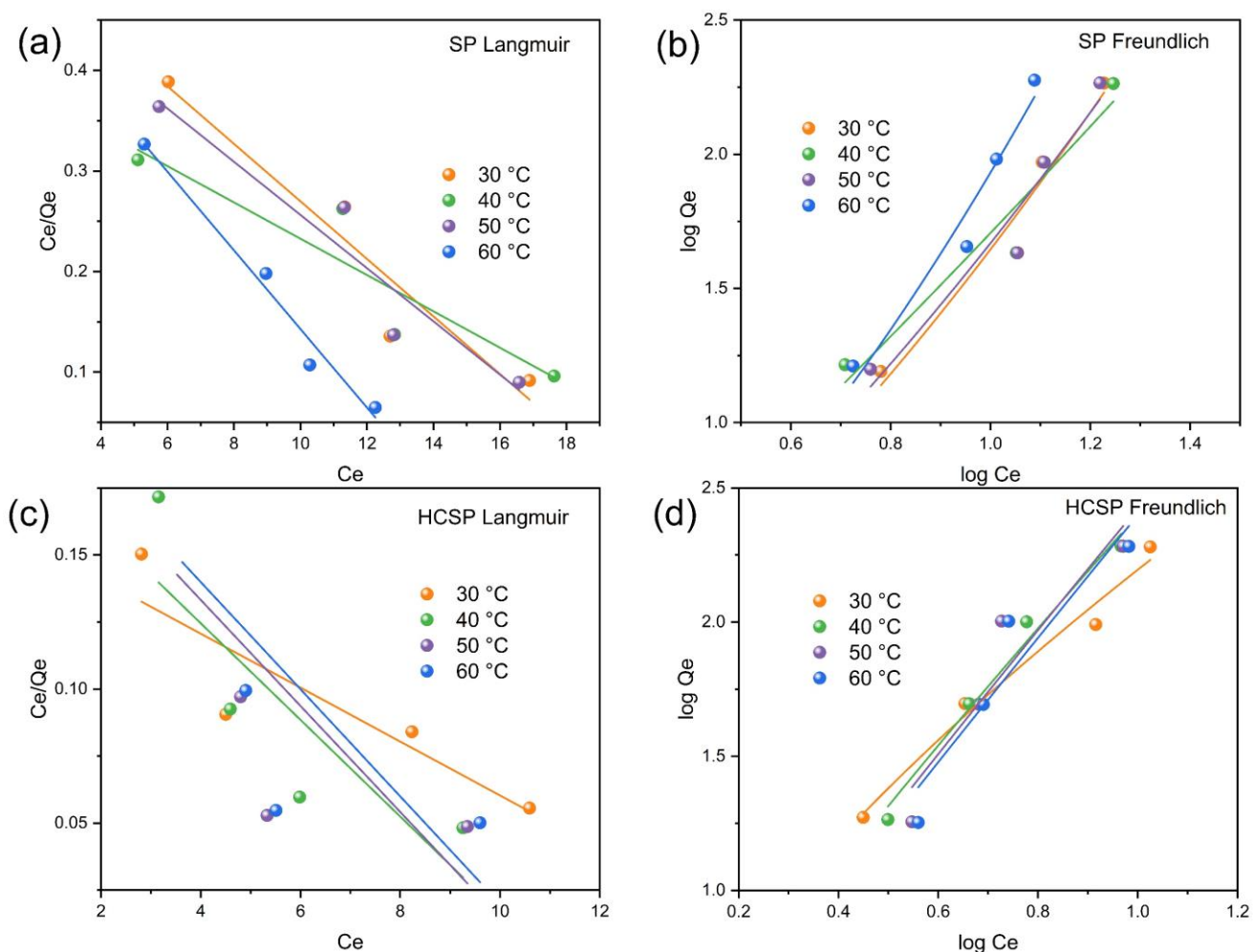


**Figure 3** The graphic of model isotherm Langmuir of SP (a) and HCSP (c), and isotherm Freundlich of SP (b) and HCSP (d).

**Table 3** The adsorption isotherm Langmuir and Freundlich parameter of SP and HCSP.

Adsorbent	T (°C)	Langmuir			Freundlich		
		$Q_{max}$	$kL$	$R^2$	$n$	$kF$	$R^2$
SP	30	34.96	0.051	0.913	0.420	5.158	0.944
	40	55.25	0.044	0.844	0.527	1.525	0.927
	50	37.74	0.051	0.915	0.443	3.725	0.933
	60	25.57	0.075	0.977	0.443	3.725	0.948
HCSP	30	99.01	0.063	0.794	0.610	3.645	0.980
	40	55.56	0.092	0.714	0.456	1.651	0.979
	50	50.50	0.093	0.529	0.426	1.230	0.889
	60	50.00	0.091	0.530	0.424	1.130	0.892

Adsorption thermodynamic data of SP and HCSP adsorbents at the initial concentration of 200 mg/L gave the evidence that both adsorption processes are endothermic because of the positive enthalpy ( $\Delta H$ ) values of 9.070 kJ/mol for SP and 2.612 kJ/mol for HCSP, respectively; hence, adsorption on both materials needs energy absorption from surroundings, and the greater the temperature, the greater is the tendency for adsorption on it. The positive entropy  $\Delta S$  values represent increasing disorder at the adsorbent-adsorbate interface of 0.049 kJ/mol·K for SP and 0.033 kJ/mol·K for HCSP and can thus be interpreted as the disorder created in water

molecules released from the adsorbent surface during the binding of the adsorbate. Also, all negative values obtained for  $\Delta G$  at different temperatures for the two adsorbents suggest that adsorption spontaneous. At every temperature considered in this study, HCSP showed more negative  $\Delta G$  values than SP, indicating thereby that adsorption on HCSP is more favorable compared to SP. However, the lower values of  $\Delta H$  for HCSP suggest that the interactions on its surface may result in weaker physical bonds in comparison with SP, albeit with a higher affinity of HCSP towards the adsorbate.

**Table 4** The adsorption thermodynamic parameters of SP and HCSP.

Adsorbent	Concentration (mg/L)	$\Delta H$ (kJ/mol)	$\Delta S$ (kJ/mol)	$\Delta G$ (kJ/mol)			
				30 °C	40 °C	50 °C	60 °C
SP	200	9.070	0.049	-5.79	-6.28	-6.77	-7.26
HCSP	200	2.612	0.033	-7.38	-7.71	-8.04	-8.37

### 3.5. Regeneration cycles

The regeneration adsorption data shows that the HCSP material adsorbs a higher percentage of malachite green dye than the SP material. Both HCSP and SP materials can be reused up to the 4<sup>th</sup> cycle, with adsorption percentages of 69.37% and 49.30%, respectively. In the first cycle, HCSP achieves a higher adsorption percentage (91.69%) compared to SP (80.14%). In the 5<sup>th</sup> cycle, the adsorption decline for HCSP (46.48%) is less than for SP (27.88%). This data suggests that the hydrochar HCSP material has better adsorption and regeneration capabilities, indicating its successful synthesis.

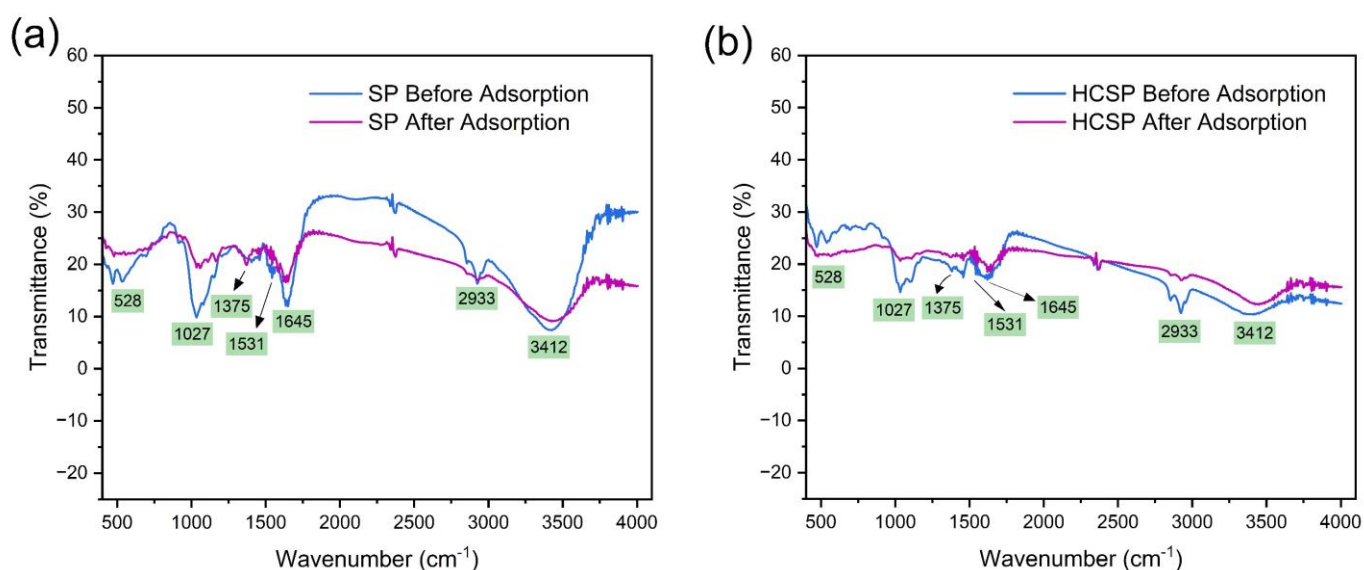
### 3.6. Study after adsorption of materials

Figure 4 shows the FTIR spectra before and after adsorption for SP (a) and HCSP (b). After adsorption of malachite green, the peaks in the FTIR spectrum decreased in intensity and shifted slightly. This indicates an interaction between the functional groups of SP and HCSP with the dye molecule. A decrease in peak intensity suggests that functional groups such as O-H, N-H, C=O, and C-OH in algae are involved in bond formation or interaction, so that their free vibrations are reduced. A peak shift indicates a change in the chemical environment around the group, which can be caused by modifications in electron distribution due to the formation of new bonds. Based on the chemical structure of malachite green, the possible bonds formed include hydrogen bonds between O-H or N-

H groups in SP and HCSP materials with amino or nitrogen groups in malachite green, electrostatic interaction between negatively charged groups in SP and HCSP with positively charged groups in malachite green, and  $\pi$ - $\pi$  interactions between the aromatic structure of malachite green with phenolic groups in SP and HCSP [31, 32]. This decrease in peak intensity and shift indicates successful adsorption, where functional groups on the surface of SP and HCSP materials actively interact with malachite green, making SP and HCSP materials effective adsorbents for malachite green dye. Figure 5 shows possible adsorption mechanisms that occur in SP and HCSP materials with malachite green dyes.

## 4. Limitation

This study shows that the regeneration of hydrochar from *Spirogyra sp.* still has limitations, especially in maintaining adsorption capacity after several cycles of use. This decrease indicates the need for further analysis of the adsorbent life cycle to identify the optimal point of regeneration before the adsorbent loses its efficiency significantly. In addition, investigation into alternative materials or material blends could be a potential solution to improve the durability of the hydrochar structure during the regeneration process. With this approach, not only can the adsorption capacity be maintained, but also the useful life of the adsorbent can be extended, thus improving its efficiency and sustainability.

**Figure 4** The FTIR spectra before and after adsorption of SP (a) and HCSP (b).

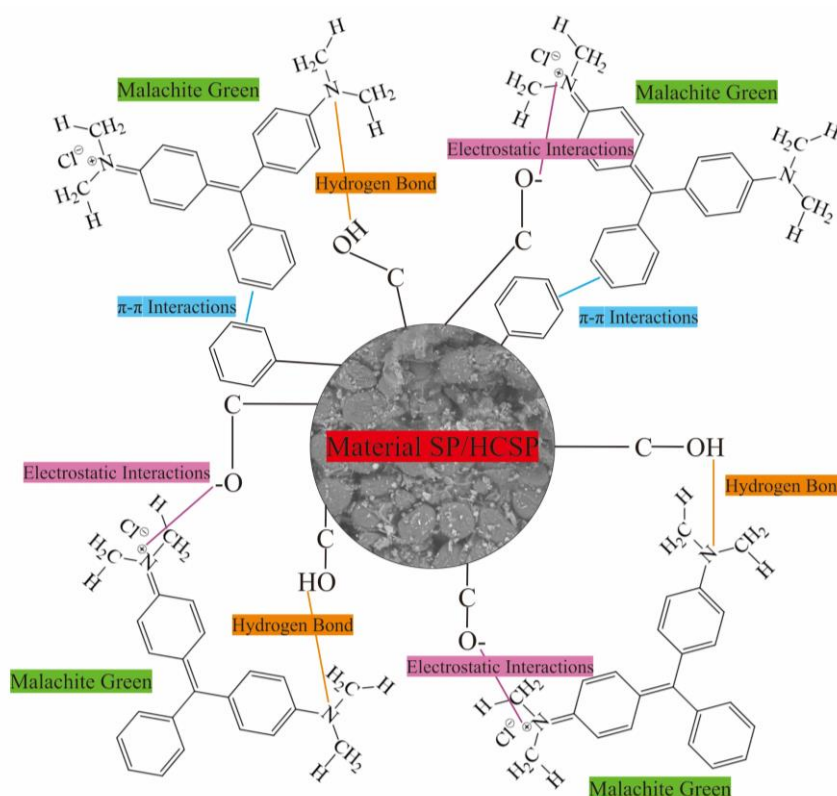


**Figure 5** Possible adsorption mechanisms that occur in SP and HCSP materials with malachite green dyes.

## 5. Conclusions

Hydrochar from *Spirogyra sp.* algae (HCSP) prepared through hydrothermal carbonization demonstrated better adsorption and regeneration abilities compared to pure *Spirogyra sp.* algae (SP). FTIR analysis confirmed the successful preparation of HCSP, with the removal of water and phenolic groups. XRD analysis indicated that HCSP has a phase similar to  $\text{CaCO}_3$  and highlighted an increase in carbon ratio with a more structured arrangement, supported by SEM data showing a regular morphology of HCSP in the form of porous granules. EDS data supported the previous findings, showing an increase in the percentage of C atoms in HCSP. The suitable adsorption kinetics model was PSO, and the adsorption isotherm model tended to follow the Freundlich model. The maximum adsorption capacity ( $Q_{\text{max}}$ ) obtained from the Langmuir calculation at 30 °C for SP and HCSP was 34.96 mg/g and 99.01 mg/g, respectively. Thermodynamic parameters indicated endothermic and spontaneous processes, with HCSP exhibiting greater adsorption capacity and spontaneity than SP. The materials after adsorption of malachite green dye show the hydrogen bond interactions,  $\pi$ - $\pi$  bonds and electrostatic interactions seen in the results of FTIR analysis, which indicates that SP and HCSP materials are suitable for adsorbing malachite green dye. Regeneration studies on HCSP and SP materials showed they could be reused up to the 4<sup>th</sup> cycle with remaining efficiency of 69.37% and 49.30%, respectively. The better reusability and improved adsorption capacity of HCSP over SP demonstrate the success of this study.

## Supplementary materials

No supplementary materials are available.

## Acknowledgments

Thank you for Research Center of Inorganic Materials and Coordination Complexes Universitas Sriwijaya to support this research.

## Author contributions

Conceptualization: M.B., A.L., L.H., E.M.  
 Data curation: M.B., S.W.  
 Formal Analysis: M.B., S.W.  
 Funding acquisition: M.B., A.L.  
 Investigation: M.B., A.L., S.W.  
 Methodology: M.B., A.L., L.H., E.M., S.W.  
 Project administration: M.B., A.L., L.H., E.M., S.W.  
 Resources: M.B., S.W.  
 Software: M.B., S.W.  
 Supervision: A.L., L.H., E.M.  
 Validation: A.L., L.H., E.M.  
 Visualization: M.B., S.W.  
 Writing - original draft: M.B., S.W.  
 Writing - review & editing: M.B., A.L., L.H., E.M., S.W.

## Conflict of interest

The authors declare no conflict of interest.

## Additional information

Authors IDs:

Muhammad Badaruddin, Scopus ID [57947818600](https://orcid.org/57947818600);  
 Laila Hanum, Scopus ID [57194601647](https://orcid.org/57194601647);  
 Elda Melwita, Scopus ID [57197848364](https://orcid.org/57197848364);  
 Sahrul Wibiyana, Scopus ID [58238186100](https://orcid.org/58238186100);  
 Aldes Lesbani, Scopus ID [15056199800](https://orcid.org/15056199800).

Website:

Universitas Sriwijaya, <https://www.unsri.ac.id/>.



## References

- Rai N, Sinha DK, Soni S, et al. Biosorption study of basic dye using aerial part of widely growing weed *Chenopodium album*. *Desalination Water Treat.* 2023;314:276–285. doi:[10.5004/dwt.2023.301122](https://doi.org/10.5004/dwt.2023.301122)
- Patel A, Soni S, Mittal J, Mittal A, Arora C. Sequestration of crystal violet from aqueous solution using ash of black turmeric rhizome. *Desalination Water Treat.* 2021;220:342–352. doi:[10.5004/dwt.2021.26911](https://doi.org/10.5004/dwt.2021.26911)
- Soni S, Bajpai PK, Mittal J, Arora C. Utilisation of cobalt doped Iron based MOF for enhanced removal and recovery of methylene blue dye from waste water. *J Mol Liq.* 2020;314. doi:[10.1016/j.molliq.2020.113642](https://doi.org/10.1016/j.molliq.2020.113642)
- Arora C, Kumar P, Soni S, Mittal J, Mittal A, Singh B. Efficient removal of malachite green dye from aqueous solution using curcuma caesia based activated carbon. *Desalination Water Treat.* 2020;195:341–352. doi:[10.5004/dwt.2020.25897](https://doi.org/10.5004/dwt.2020.25897)
- Kumar A, Singh R, Kumar Upadhyay Sanjay Kumar S, Charaya MU. Biosorption: The Removal of Toxic Dyes from Industrial Effluent Using Phytobiomass- A Review. *Plant Arch.* 2021;21(1):1320–1325. doi:[10.51470/plantarchives.2021.v21.s1.207](https://doi.org/10.51470/plantarchives.2021.v21.s1.207)
- Shabir M, Yasin M, Hussain M, et al. A review on recent advances in the treatment of dye-polluted wastewater. *J Industr Eng Chem.* 2022;112:1–19. doi:[10.1016/j.jiec.2022.05.013](https://doi.org/10.1016/j.jiec.2022.05.013)
- Mondal MIH, Hossen A, Chowdhury T. Purification of textile dye-contaminated wastewater by three alternative promising techniques: Adsorption, Biodegradation and Advanced Oxidation Processes (AOPs) - A review. *J Textile Eng Fashion Technol.* 2022;8(3):96–98. doi:[10.15406/jteft.2022.08.00306](https://doi.org/10.15406/jteft.2022.08.00306)
- Gallego-Ramirez C, Chica E, Rubio-Clemente A. Coupling of Advanced Oxidation Technologies and Biochar for the Removal of Dyes in Water. *Water (Switzerland).* 2022;14(16):1–24. doi:[10.3390/w14162531](https://doi.org/10.3390/w14162531)
- Goswami L, Kushwaha A, Kafle SR, Kim BS. Surface Modification of Biochar for Dye Removal from Wastewater. *Catalysts.* 2022;12(8). doi:[10.3390/catal12080817](https://doi.org/10.3390/catal12080817)
- Xie LQ, Jiang XY, Yu JG. A Novel Low-Cost Bio-Sorbent Prepared from Crisp Persimmon Peel by Low-Temperature Pyrolysis for Adsorption of Organic Dyes. *Molecules.* 2022;27(16). doi:[10.3390/molecules27165160](https://doi.org/10.3390/molecules27165160)
- Hessien M. Methylene Blue Dye Adsorption on Iron Oxide-Hydrochar Composite Synthesized via a Facile Microwave-Assisted Hydrothermal Carbonization of Pomegranate Peels' Waste. *Molecules.* 2023;28(11). doi:[10.3390/molecules28114526](https://doi.org/10.3390/molecules28114526)
- Zhou Y, Lu J, Zhou Y, Liu Y. Recent advances for dyes removal using novel adsorbents: A review. *Environ Pollution.* 2019;252:352–365. doi:[10.1016/j.envpol.2019.05.072](https://doi.org/10.1016/j.envpol.2019.05.072)
- Farghal HH, Nebsen M, El-Sayed MMH. Exploitation of expired cellulose biopolymers as hydrochars for capturing emerging contaminants from water. *RSC Adv.* 2023;13(29):19757–19769. doi:[10.1039/d3ra02965d](https://doi.org/10.1039/d3ra02965d)
- Adamović A, Petronijević M, Panić S, et al. Biochar and hydrochar as adsorbents for the removal of contaminants of emerging concern from wastewater. *Adv Technol.* 2023;12(1):57–74. doi:[10.5937/savteh2301057a](https://doi.org/10.5937/savteh2301057a)
- Rodriguez Correa C, Hehr T, Voglhuber-Slavinsky A, Rauscher Y, Kruse A. Pyrolysis vs. hydrothermal carbonization: Understanding the effect of biomass structural components and inorganic compounds on the char properties. *J Anal Appl Pyrolysis.* 2019;140:137–147. doi:[10.1016/j.jaap.2019.03.007](https://doi.org/10.1016/j.jaap.2019.03.007)
- Cavali M, Libardi Junior N, de Sena JD, et al. A review on hydrothermal carbonization of potential biomass wastes, characterization and environmental applications of hydrochar, and biorefinery perspectives of the process. *Sci Total Environ.* 2023;857. doi:[10.1016/j.scitotenv.2022.159627](https://doi.org/10.1016/j.scitotenv.2022.159627)
- Chand V, Vanavana I. Evaluation of *Spirogyra* Sp. as a Bioindicator of Heavy metal Pollution in a Tropical Aquatic Environment. *Pollut Res.* Published online June 30, 2022:445–450. doi:[10.53550/pr.2022.v4i102.009](https://doi.org/10.53550/pr.2022.v4i102.009)
- Demiriz Yücer T. Investigation of *Spirogyra daedaleoides* *Czruda* in terms of bioactive components. *Ege J Fisheries Aquatic Sci.* 2024;41(2):142–147. doi:[10.12714/egejfas.41.2.07](https://doi.org/10.12714/egejfas.41.2.07)
- Tipnee S, Unpaprom Y, Ramaraj R, Tipnee S, Ramaraj R, Unpaprom Y. Nutritional Evaluation of Edible Freshwater Green Macroalga *Spirogyra* varians. *Emer Life Sci Res.* 2015;1(2):1–7.
- Siri-anusornsak W, Kolawole O, Soiklom S, et al. Innovative Use of *Spirogyra* sp. Biomass for the Sustainable Adsorption of Aflatoxin B1 and Ochratoxin A in Aqueous Solutions. *Molecules.* 2024;29(21). doi:[10.3390/molecules29215038](https://doi.org/10.3390/molecules29215038)
- Permann C, Gierlinger N, Holzinger A. Zygospores of the green alga *Spirogyra*: new insights from structural and chemical imaging. *Front Plant Sci.* 2022;13. doi:[10.3389/fpls.2022.1080111](https://doi.org/10.3389/fpls.2022.1080111)
- Aksu A, Kütük N, Çaylak O, et al. Theoretically supported experimental analyses on Safranin O biosorption from textile wastewater via dead biomass of *Spirogyra porticalis*. *Biomass Convers Biorefin.* Published online 2024. doi:[10.1007/s13399-024-05882-x](https://doi.org/10.1007/s13399-024-05882-x)
- Lesbani A, Ahmad N, Mohadi R, et al. Selective adsorption of cationic dyes by layered double hydroxide with assist algae (*Spirulina platensis*) to enrich functional groups. *JCIS Open.* 2024;15. doi:[10.1016/j.jciso.2024.100118](https://doi.org/10.1016/j.jciso.2024.100118)
- Djezzar Z, Aidi A, Rehali H, Ziad S, Othmane T. Characterization of activated carbon produced from the green algae *Spirogyra* used as a cost-effective adsorbent for enhanced removal of copper(ii): application in industrial wastewater treatment. *RSC Adv.* 2024;14(8):5276–5289. doi:[10.1039/d3ra08678j](https://doi.org/10.1039/d3ra08678j)
- Guleria S, Chawla P, Relhan A, Kumar A, Bhasin A, Zhou JL. Antibacterial and photocatalytic potential of bioactive compounds extracted from freshwater microalgae species (*Spirogyra* and *Oocillatoria*): A comparative analysis. *Sci Total Environ.* 2024;912. doi:[10.1016/j.scitotenv.2023.169224](https://doi.org/10.1016/j.scitotenv.2023.169224)
- Masoumi S, Dalai AK. Optimized production and characterization of highly porous activated carbon from algal-derived hydrochar. *J Clean Prod.* 2020;263. doi:[10.1016/j.jclepro.2020.121427](https://doi.org/10.1016/j.jclepro.2020.121427)
- Taher T, Maulana S, Mawaddah N, Munandar A, Rianjanu A, Lesbani A. Low-temperature hydrothermal carbonization of activated carbon microsphere derived from microcrystalline cellulose as carbon dioxide (CO<sub>2</sub>) adsorbent. *Mater Today Sustainability.* 2023;23. doi:[10.1016/j.mtsust.2023.100464](https://doi.org/10.1016/j.mtsust.2023.100464)
- Gibson N, Kuchenbecker P, Rasmussen K, Hodoroaba VD, Rauscher H. Volume-specific surface area by gas adsorption analysis with the BET method. In: *Characterization of Nanoparticles: Measurement Processes for Nanoparticles.* Elsevier; 2019:265–294. doi:[10.1016/B978-0-12-814182-3.00017-1](https://doi.org/10.1016/B978-0-12-814182-3.00017-1)
- Li W, Tao E, Hao X, Li N, Li Y, Yang S. MMT and ZrO<sub>2</sub> jointly regulate the pore size of graphene oxide-based composite aerogel materials to improve the selective removal ability of Cu(II). *Sep Purif Technol.* 2024;331. doi:[10.1016/j.seppur.2023.125506](https://doi.org/10.1016/j.seppur.2023.125506)
- Smječanin N, Bužo D, Mašić E, et al. Algae based green biocomposites for uranium removal from wastewater: Kinetic, equilibrium and thermodynamic studies. *Mater Chem Phys.* 2022;283. doi:[10.1016/j.matchemphys.2022.125998](https://doi.org/10.1016/j.matchemphys.2022.125998)
- Soni S, Bajpai PK, Bharti D, Mittal J, Arora C. Removal of crystal violet from aqueous solution using iron based metal organic framework. *Desalination Water Treat.* 2020;205:386–399. doi:[10.5004/dwt.2020.26387](https://doi.org/10.5004/dwt.2020.26387)
- Lesbani A, Ahmad N, Wibiyan S, et al. Improving congo red dye removal by modification layered double hydroxide with microalgae and macroalgae: Characterization and parametric optimization. *Colloids Surf A Physicochem Eng Asp.* 2025;706. doi:[10.1016/j.colsurfa.2024.135770](https://doi.org/10.1016/j.colsurfa.2024.135770)